Ocean alkalinity enhancement approaches and the predictability of runaway precipitation processes -

Results of an experimental study to determine critical alkalinity ranges for safe and sustainable application scenarios

Niels Suitner[1], Giulia Faucher[2], Carl Lim[3], Julieta Schneider[2], Charly A. Moras[4], Ulf Riebesell[2] and Jens Hartmann[1]

[1]Institute for Geology, Universität Hamburg, Bundesstrasse 55, 20146 Hamburg, Germany

[2]GEOMAR Helmholtz Centre for Ocean Research Kiel, Wischhofstrasse 1-3, 24148 Kiel, Germany

[3]KU Leuven, Bruges, Department of Materials Engineering, B-8200, Belgium

[4]Faculty of Science and Engineering, Southern Cross University, Lismore, NSW 2480, Australia

Correspondence: Niels Suitner (niels.suitner@uni-hamburg.de), Jens Hartmann (geo@hattes.de)

Orcid:

Niels Suitner:	https://orcid.org/0000-0003-3413-857X
Giulia Faucher:	https://orcid.org/0000-0001-8930-477X
Carl Lim:	https://orcid.org/0000-0002-9035-4771
Julieta Schneider:	https://orcid.org/0000-0002-7271-717X
Charly A. Moras:	https://orcid.org/0000-0001-6819-6167
Ulf Riebesell:	https://orcid.org/0000-0002-9442-452X
Jens Hartmann:	https://orcid.org/0000-0003-1878-9321

Abstract

To ensure the safe and efficient application of Ocean Alkalinity Enhancement (OAE), it is crucial to investigate its impacts on the carbonate system. While modeling studies reported a sequestration potential of 3-30 Gt CO_2 per year (Oschlies et al., 2023), there has been a lack of empirical data to support the applicability of this technology in natural environments. Recent studies have described the effect of runaway carbonate precipitation in the context of OAE, showing that calcium carbonate formation was triggered if certain $\Omega_{aragonite}$ saturation thresholds were exceeded. This effect could potentially lead to a net loss of the initially added alkalinity, counteracting the whole concept of OAE. The related precipitation can adversely affect the carbon storage capacity and may in some cases result in CO_2 emissions. Experiments at the Espeland Marine Biological Station (Bergen, Norway) were conducted to systematically study the chemical consequences of OAE deployment. The experiments lasted for 20-25 days to monitor the temporal development of carbonate chemistry parameters after alkalinity addition and the eventually triggered carbonate precipitation process. Identified uniform patterns before and during the triggered runaway process can be described by empirical functional relationships. For approaches equilibrated to the CO_2 concentration of the atmosphere, total alkalinity levels (TA) of up to 6500 μmol kg^{-1} remained stable without loss of total alkalinity (TA) for up to 20 days. Higher implemented TA levels, up to 11200 μmol kg^{-1}, triggered runaway carbonate formation. Once triggered, the loss of alkalinity continued until the $\Omega_{aragonite}$ values leveled out at 5.8-6.0, still resulting in a net gain of 3600-4850 μmol kg^{-1} in TA. The non-CO_2-equilibrated approaches, however, remained only stable for TA additions of up to 1000 μmol kg^{-1}. The systematic behavior of treatments exceeding this level allows to predict the duration of transient stability and the quantity of TA loss after this period. Once triggered, the TA-loss continued in the non-CO_2-equilibrated approaches until $\Omega_{aragonite}$ values of 2.5–5.0 were reached, in this case resulting in a net loss of TA. To prevent a net loss of TA, treated water must be diluted below the time-dependent critical levels of TA and $\Omega_{aragonite}$ within the identified transient stability duration. Identified stability and loss patterns of added TA depend on local environmental conditions impacting the carbonate system, like salinity, temperature, biological activity, and particle abundance. Incorporating such stability and loss patterns into ocean biogeochemical models, which are capable of resolving dilution processes of treated and untreated water parcels, would, from a geochemical perspective, facilitate the prediction of safe local application levels of OAE. This approach would also allow for an accurate determination of the fate of added alkalinity and a more realistic carbon storage potential estimation compared to the assessments that neglect carbonate system responses to OAE.

1 Introduction

At the current greenhouse gas emission rates, global warming well below 2°C, compared to pre-industrial levels, as targeted by the Paris Agreement (UNFCCC, 2015) might not be achievable (Meinshausen et al., 2009; Rogelj et al., 2016). To prevent such a development, international efforts have turned the spotlight on reducing greenhouse gas emissions globally. However, to comply with the climate goals, greater attention needs to be paid to carbon dioxide removal (CDR) technologies. One such marine-based technology is ocean alkalinity enhancement (OAE), a strategy that aims to chemically sequester carbon dioxide (CO_2) as carbonate (CO_3^{2-}) or bicarbonate (HCO_3^-) ions in ocean water (Kheshgi, 1995; NASEM, 2022). The concept of OAE strives to increase the inorganic carbon storage capacity by increasing the total alkalinity (TA) of seawater (Caldeira & Rau, 2000; Hartmann et al., 2013; Köhler et al., 2010; Schuiling & Krijgsman, 2006). Naturally, inorganic carbon is stored in the ocean over periods of time ranging from 10,000 to 100,000 years (Berner et al., 1983; Mackenzie & Garrels, 1966). This long-term carbon storage potential makes OAE a preferred option over other suggested marine CDR methods. Naturally, inorganic carbon is stored in the ocean over periods of time ranging from 10,000 to 100,000 years (Berner et al., 1983; Mackenzie & Garrels, 1966). This long-term carbon storage potential makes OAE a preferred option over other suggested marine CDR methods. An accompanying benefit of this strategy is the parallel increase in pH, thus counteracting ocean acidification (Ilyina et al., 2013; Köhler et al., 2010).

Tests for OAE under close-to-natural conditions are still scarce (Albright et al., 2016; Cyronak et al., 2023; Ferderer et al., 2022; Paul et al., 2023; Sánchez et al., 2023; Yang et al., 2023). For a safe and efficient application of OAE, it is crucial to assess the induced changes in carbonate chemistry and investigate their potential environmental impacts (Bach et al., 2019; Riebesell et al., 2023).

In isolated case studies, prototypes for alkalinity enhancement have already been put into practice to counteract lake acidification (e.g., Koch & Mazur, 2016; LMBV, 2017) or were discussed in context of river water alkalinity enhancement (Sterling et al., 2023). Various application methods for OAE ranging from spreading ground rock powder or mineral phases (Kheshgi, 1995) to liquid addition of alkaline solutions directly into the seawater or via rivers (Hartmann et al., 2013; Sterling et al., 2023), and electrochemical alkalinity generation (Eisaman et al., 2023; Renforth & Henderson, 2017) have been proposed. Alkalinity enhancement could be achieved in a CO_2-equilibrated or non-CO_2-equilibrated manner, as discussed in Schulz et al. (2023). In the non-equilibrated scenario, the seawater would gradually equilibrate over time by absorbing atmospheric CO_2. The CO_2-equilibrated approach consists of adding alkalized water that is already in equilibrium with the atmosphere. This means that at the point of addition, the water is put into equilibrium with the atmosphere either with technological apparatus before release or a CO_2 source is used to bring the water into equilibrium after TA addition.

81 Alternatively, solids like Na_2CO_3 or $NaHCO_3$ could be used for OAE since they are already used to capture CO_2 from a source
82 (e.g., Forster 2012, 2014) before the alkaline products are disposed of.
83 To illustrate the impact of different alkalinity addition scenarios on various carbonate chemistry parameters, Figure 1 presents
84 a TA:DIC diagram modelled after Deffeyes (1965). Besides dissolved inorganic carbon (DIC) and total alkalinity, the Deffeyes
85 diagram provides information on corresponding pH, pCO_2, and saturation state for aragonite ($\Omega_{aragonite}$).
86 Surpassing critical thresholds of $\Omega_{aragonite}$ saturation states for a certain period of time could result in $CaCO_3$ precipitation
87 (Schulz et al., 2023; Zeebe & Wolf-Gladrow, 2001). This phenomenon could lead to a runaway process, as observed in
88 laboratory-based experimental studies conducted by Moras et al. (2022), Hartmann et al. (2023), Fuhr et al. (2022), and Pan
89 et al. (2021). This process could lead to a net loss in CO_2-storage potential and will result in a leakage of TA and DIC.
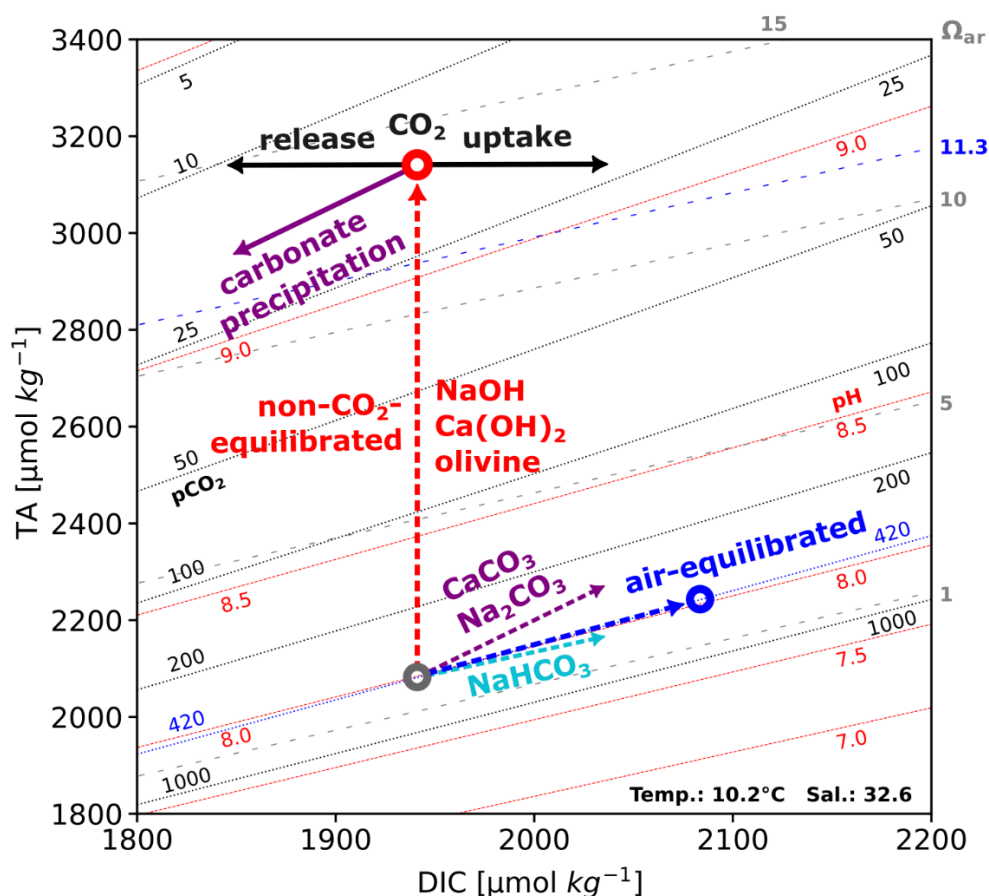

Figure 1: Example of a TA:DIC diagram after Deffeyes, 1965, in context of OAE; background contours represent iso-lines
of pH (red), $\Omega_{aragonite}$ (dotted grey) and pCO_2 (black) values; shown contours reflect pH, pCO_2 and $\Omega_{aragonite}$ values for varying
TA and DIC levels at given temperature and salinity conditions; dashed arrows show the impact of indicated alkalinization

4

approaches, e.g. non-CO_2-equilibrated TA addition could be realized by injection or dissolution of sodium hydroxide (NaOH), an air-equilibrated TA addition (in an equilibrium to the atmosphere – pCO_2 420 µatm) could be achieved by utilizing a combination of $NaHCO_3$ and Na_2CO_3; during non-CO_2-equilibrated approaches the pCO_2 of the manipulated water is reduced, creating the potential of CO_2 uptake (black arrow) from the atmosphere; if the TA addition surpasses certain critical ranges (for surface free waters under the given conditions here indicated by the blue $\Omega_{aragonite}$ contour of 11.3, calculated after Marion et al. (2009)), carbonate precipitation (purple arrow) results in the reverse changes of $CaCO_3$ dissolution

90   Considering the complexity and variety of possible environmental impacts of OAE scenarios, systematic empirical
91   investigations of alkalinization approaches seem to be vital providing meaningful sustainability assessments. This study aims
92   to assess the geochemical impacts of alkalinity addition in seawater by refining and improving upon the experimental setup of
93   Hartmann et al. (2023), testing CO_2-equilibrated and non-equilibrated TA enhancement scenarios in natural seawater.
94   Incubation experiments were conducted with extended TA ranges and runtimes, along with increased sampling frequency and
95   enhanced resolution of the TA gradients. Experiments were designed to identify stability ranges of the added alkalinity and
96   characterize critical thresholds that trigger the runaway precipitation process.

2 Methods

2.1 Experimental setup

Four sets of experiments were conducted between May and July 2022 using natural seawater from the Raunefjord (60.27°N, 5.20°E) close to the Espeland Marine Biological Station (Bergen, Norway). All four experiments used the same setup. 250 ml polystyrene cell culture bottles were filled with filtered seawater in a flow-through incubation box (PMMA) and incubated outdoors to follow the local light conditions (see Fig. S1). The box was covered in blue foil (172 Lagoon Blue foil, Lee filters, Burbank, CA, United States) to mimic the light conditions in the fjord at a depth of ~5 m. The temperature was regulated by recirculating fjord water in the incubation box, thus ensuring that the incubation temperature matched that of the fjord. To prevent the occurrence of substantial headspace throughout the experiment, each treatment level was divided into 3-4 separate bottles. The division allowed for progressive volume removal during sampling while reducing the potential for gas exchange processes. Within each experiment, a new set of bottles was opened sequentially after 3-4 samplings. Alkalinity was enhanced using a 0.5 M NaOH (sodium hydroxide) stock solution for the non-CO_2-equilibrated and a combination of $NaHCO_3$ (sodium bicarbonate, 0.4 M) and Na_2CO_3 (sodium carbonate, 0.2 M) stock solutions for the preparation of the CO_2-equilibrated treatments. The latter were adjusted to attain equilibrium with the surrounding air's CO_2 concentration (~420 µatm). For each of the two, the experimental setups encompassed: 1. abiotic conditions, achieved by removing organisms via filtration through a 0.2 µm filter, 2. biotic where only the small phytoplankton community was included by using a 50 µm filter mesh to remove larger particles and organisms. The categorization into abiotic and biotic treatments aimed to determine the potential influences of biological activity or naturally occurring sediments, while also preserving the comparability of the experimental setup described in Hartmann et al. (2023). An overview of the reached TA-levels and step sizes, runtimes and temperature ranges is given in Table 1. The experiments were conducted over a span of two months, with each incubation run for 20 or 25 days. The experiments were therefore partially separated in time, resulting in slight variations in starting conditions and average temperatures, ranging from 10 to 16°C. Biotic and abiotic treatments were simultaneously conducted within each equilibration mode. The initial carbonate chemistry parameters of the collected seawater before manipulation were relatively constant for all approaches (TA$_{initial}$ ~2190 ± 10 µmol kg^{-1}, DIC ~1890 ± 20 µmol kg^{-1}, pH ~8.25 ± 0.05, Sal. ~32.6 ± 0.1).

Table 1: Overview experimental design Bergen 2022

#	Seawater conditions	CO_2 state to atmosphere	Alkaline material	Runtime [days]	Range TA_{added} [μmol kg^{-1}]	TA_{added} gradient steps [μmol kg^{-1}]	Temperature [°C]
I	biotic	air-equilibrated	$Na_2CO_3/$ $NaHCO_3$	20	0-2800	200	12-15
	abiotic			20	0-9200	200/800	12-16
II	biotic	non-equilibrated	NaOH	25	0-2800	200	10-11
	abiotic			25	0-3400	200	11-13

2.2 Sampling and measurements

For carbonate chemistry analysis, 40-50 ml of incubated water were taken per sampling day and treatment level. Using a peristaltic pump connected to a 0.2 µm syringe filter, samples were filtered immediately to stop further reactions, remove particles and prepare each sample for measurements. All treatments were measured without replicates for TA, pH, temperature and salinity, and biotic treatments were further analysed to assess the biological responses. An accompanying publication is going to describe the impact of enhanced alkalinity on the included phytoplanktonic communities during the first 6 days of the biotic incubation experiments. A selection of filtrates was saved for scanning electron microscopy (SEM) analysis. Minor shifts in pH, DIC and $\Omega_{aragonite}$ originate from increasing water temperatures during the runtimes of the experiments, photosynthetic activity in the biotic approaches or minor ingassing from the headspace of the reactor bottles (cf. Tab. S1).

Methods and devices for measuring TA, pH, temperature, and salinity were identical to experiments I and II from Hartmann et al. (2023). Total alkalinity was determined by titration with a 0.02M hydrochloric acid, using an 888 Titrando autosampler (Metrohm). TA measurements were corrected against certified reference materials (CRM batch 193), supplied by Prof. Andrew G. Dickson laboratory, Scripps Institution of Oceanography (USA). A WTW multimeter (MultiLine® Multi 3630 IDS) was used to measure pH (SenTix 940 pH-electrode), temperature and salinity (TetraCon 925 cell, Xylem). The pH-probe was calibrated with WTW buffer solutions according to NIST/PTB in four steps (1.679–9.180 at 25 °C) and corrected for seawater after Badocco et al. (2021). DIC, pCO_2 and saturation states were calculated using CO2SYS Excel version 2.5 (Pierrot et al., 2006), including error propagations based on Orr et al. (2018) (uncertainties were set to: TA ±5 µmol kg^{-1}; pH ±0.02; temperature ±0.1°C; salinity ±0.1). Constants in CO2SYS were set to Lueker et al. (2000) for K_1 and K_2, Dickson (1990) for $KHSO_4$, and Perez and Fraga (1987) for KHF and Lee et al. (2010) for $[B]_T$ Value, and the pH was calculated on the total scale.

The physical appearance of precipitated particles and their elemental composition were analyzed by two separate SEM setups: 1. Tabletop Microscope Hitachi TM4000plus (University of Hamburg) and 2. Zeiss Gemini Ultra55 Plus at (CAU Kiel), both equipped with an energy-dispersive X-ray spectroscopy (EDX) detector.

2.3 ΔTA equation

Based on the concept from Hartmann et al. (2023), the subsequent equation is utilized to simplify the characterization of reached values or alterations in TA:

$$\Delta TA_{net} = TA_{final} - TA_{initial} = \Delta TA_{added} + \Delta TA_{loss}$$

ΔTA_{net}: net change of TA

TA_{final}: absolute reached TA after TA addition (measured)

$TA_{initial}$: initial TA of used seawater (measured)

ΔTA_{added}: amount of increased TA by alkalinity addition

ΔTA_{loss}: amount of TA decline during the experiment (negative sign)

3 Results

3.1 CO₂ equilibrated experiments
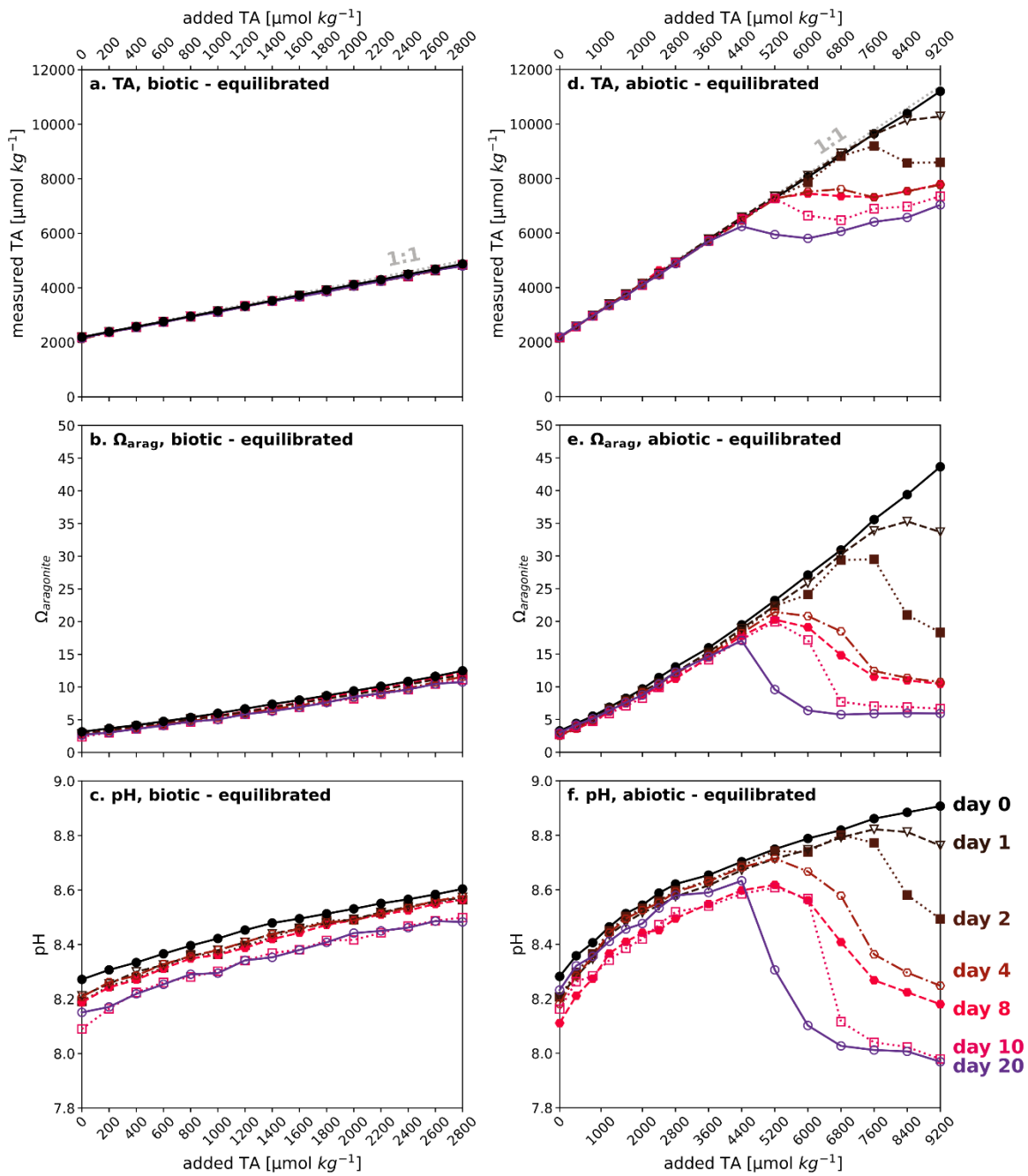
Figure 2: Temporal TA, $\Omega_{aragonite}$ and pH evolution in CO_2-equilibrated experiments, under biotic (left) and abiotic (right) conditions; each diagram represents a specific carbonate chemistry parameter investigated, i.e., measured TA (a. and d.), $\Omega_{aragonite}$ (b. and e.) and pH (c. and f.) as a function of added TA and time point; legends for sampling days are given in f; data points for days 6 and 15 have been removed to enhance the readability, related comprehensive diagrams are given in Fig. S2; in addition, temporal plots for each parameter are provided in the supplements (Fig. S5 (biotic) and S6 (abiotic)); initial conditions of the used seawater before manipulation: $TA_{initial}$ ~2190 $\mu mol\ kg^{-1}$, $\Omega_{aragonite}$ ~2.5-3.0, pH ~8.2, Sal. ~32.6, biotic: Temp. 12-15°C, abiotic: 12-16°C

158

159 In the biotic CO_2-equilibrated experiment an air-equilibrated alkalinization of up to 2800 $\mu mol\ kg^{-1}$ could be achieved during
160 the 20-day runtime. All carbonate chemistry parameters remained constant, showing that a TA addition slightly above the
161 estimated critical $\Omega_{aragonite}$ value for pseudo homogenous precipitation of 11.3 (after Marion et al., 2009) could be achieved.
162 This level was maintained for 20 days without causing any $CaCO_3$ precipitation, as illustrated in Fig. 2a-c.
163 By extending the alkalinity range up to 9200 $\mu mol\ kg^{-1}$ in the abiotic air-equilibrated experiment $\Omega_{aragonite}$ values far above
164 critical levels were reached, resulting in extensive carbonate precipitation in a runaway style (Fig. 2d-f). All targeted alkalinity
165 levels were achieved ~3min after alkalinity addition (day 0), and a decline in TA was observed in treatments above ΔTA 3600
166 (corresponding to $\Omega_{aragonite}$ of 14.6). Starting with the highest treatment levels after 1 day, precipitation was triggered in all
167 batches with a ΔTA above 3600 over the runtime of 20 days (see Fig. 2d). Following precipitation, once $\Omega_{aragonite}$ reached
168 values of 5.8-6.0, the process halted, resulting in a linear alignment of final TA values. The TA loss rate was significantly
169 reduced towards the end of the precipitation procedure; however, it could not be excluded that the process would have
170 continued if the experiment had proceeded. Despite substantial total alkalinity loss attributed to runaway precipitation, all
171 treatments involving secondary mineral formation still achieved a net gain in TA ranging from 3600 to 4850 $\mu mol\ kg^{-1}$.
172 Nevertheless, pH values in batches which underwent the precipitation process were accompanied by an acidification below
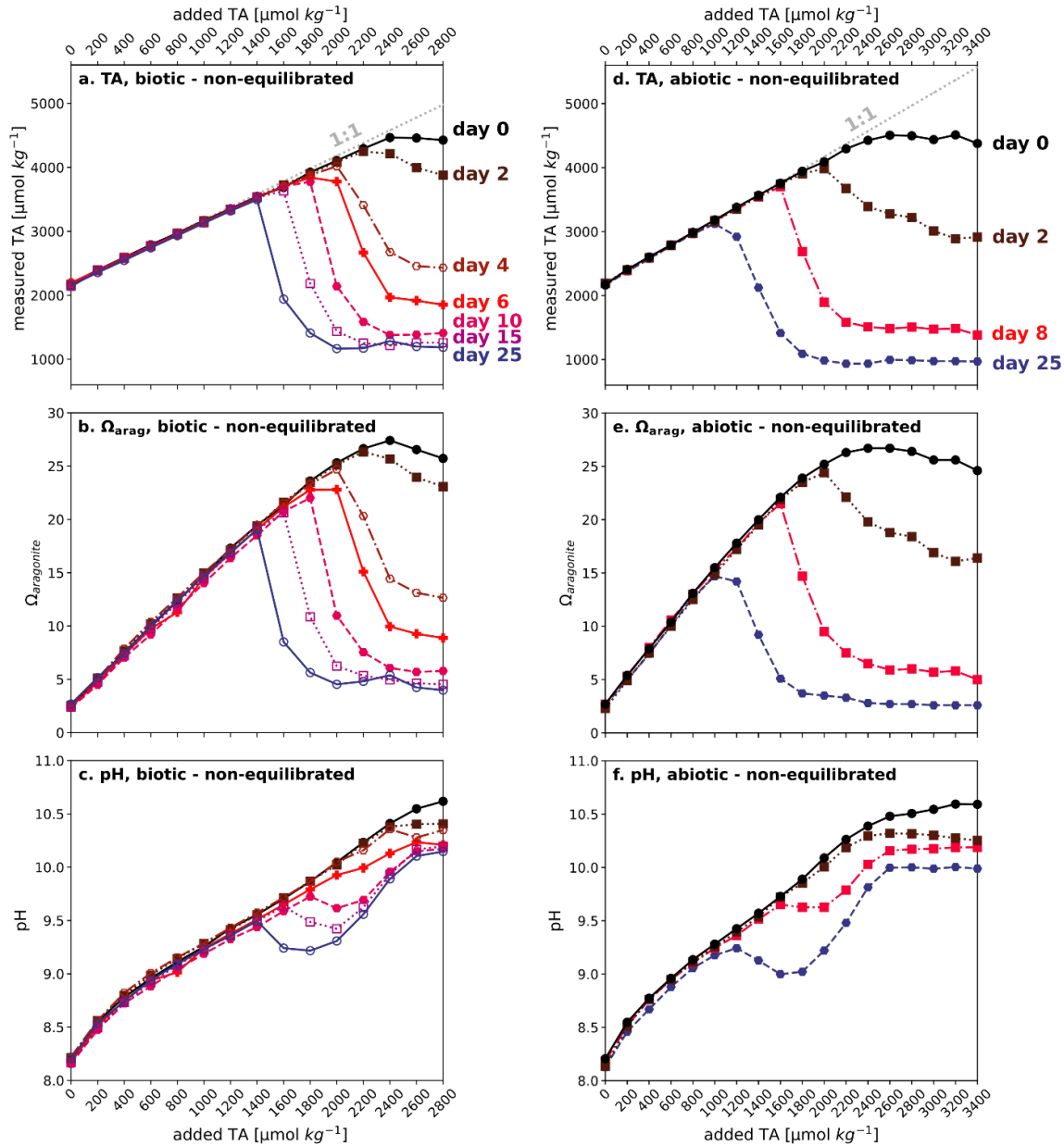173 the initial seawater pH level.

3.2 Non-CO₂-equilibrated experiments

Figure 3: TA, $\Omega_{aragonite}$ and pH evolution of non-CO₂-equilibrated experiments, biotic (left) and abiotic (right); each graph represents a specific sampling day; due to the extensive number of data points days 1 and 20 for the biotic treatments have

been removed to enhance the readability; for the abiotic approach, only a subset of data is shown; comprehensive diagrams are given in Fig. S3; in addition, temporal plots for each parameter are provided in Fig. S7 (biotic) and S8 (abiotic); initial conditions of the used seawater before manipulation: $TA_{initial}$ ~2190 µmol kg^{-1}, $\Omega_{aragonite}$ ~2.5-3.0, pH ~8.2, Sal. ~32.6, biotic: Temp. ~10-11°C, abiotic: Temp. ~11-13°C

175

176 Alkalinity enhancement in the biotic and abiotic non-CO_2-equilibrated experiments achieved a steady increase up to an addition
177 of 2400 µmol kg^{-1} at day 0 (Fig. 3). Under the given local conditions (Temp. 10-11°C, Sal. 32.6), exceeding the TA_{target} level
178 of 4570 µmol kg^{-1} led to a drop back to 4450 ± 60 µmol kg^{-1} after ~3 min, irrespective of the quantity of further added alkalinity.
179 For the biotic non-CO_2-equilibrated approach (Fig. 3a-c) treatments from ΔTA 1400 to 2800 showed a decrease in alkalinity
180 during the subsequent 25-day runtime, as a consequence of secondary mineral formation. The precipitation process uniformly
181 came to halt in a range of 1230 ± 60 µmol kg^{-1}, corresponding to an $\Omega_{aragonite}$ of 4-5. A similar behavior was observed in the
182 abiotic non-CO_2-equilibrated experiment (Fig. 3d-f). Slightly higher water temperatures (11-13°C) in comparison to the biotic
183 approach (10-11°C), potentially led to an earlier decline of alkalinity and lower final in TA (1030 ± 60 µmol kg^{-1}) and $\Omega_{aragonite}$
184 (2.5-4). All treatment levels from ΔTA 1200 to 3400 showed precipitation during the 25-day runtime. Unlike the abiotic CO_2-
185 equilibrated approach, the runaway precipitation in both non-equilibrated experiments resulted in a net-loss of alkalinity, while
186 pH values remained in a range of 9.0-10.1. Nevertheless, despite relatively high $\Omega_{aragonite}$ values of up to ~17 (biotic) and ~15
187 (abiotic) in the non-CO_2-equilibrated experiments, after 25 days the alkalinity was still constant in all treatments below ΔTA
188 1200.

189 **3.3 TA:DIC diagrams**

190 TA:DIC diagrams in Fig. 4a-e provide a contextualized overview of trend and temporal development of carbonate chemistry
191 parameters. Simultaneous TA and DIC enhancement in the CO_2-equilibrated experiments led to the characteristic diagonal
192 gradient, while non-CO_2-equilibrated approaches resulted in a straight vertical increase in TA as a consequence of OH$^-$
193 injection (also see Fig. 1). Treatments exhibiting secondary carbonate formation followed the strict 2:1-ΔTA:ΔDIC decline
194 ratio during the precipitation phase, leading to a consistent alignment of data points in straight trend trajectories. The tendency
195 for consistent linear trends in TA/DIC during alkalinization and precipitation processes in the conducted experiments, allows
196 to visually trace the origin of shapes and temporal development trends of pH and $\Omega_{aragonite}$ in Figures 2 and 3 by utilizing
197 exhibited TA:DIC diagrams. For example, the consistency of $\Omega_{aragonite}$ values within treatments that underwent the runaway
198 process allows to predict the final state of other carbonate chemistry parameters, oriented on the shape and position of the
199 related $\Omega_{aragonite}$ contour (see Fig. 4b-e). The immediate drop back to 4450 ± 60 µmol kg^{-1} in both non-CO_2-equilibrated
200 experiments showed a consistent pattern in dislocation of target and measured TA and DIC values. This pattern followed a
201 steady declining ΔTA:ΔDIC loss ratio of 4.9-2.3 from highest to lowest target alkalinity levels (Fig. 4f), indicating the
202 formation of non-carbonate-bearing secondary phases, such as $Mg(OH)_2$ (also see section 4.3).

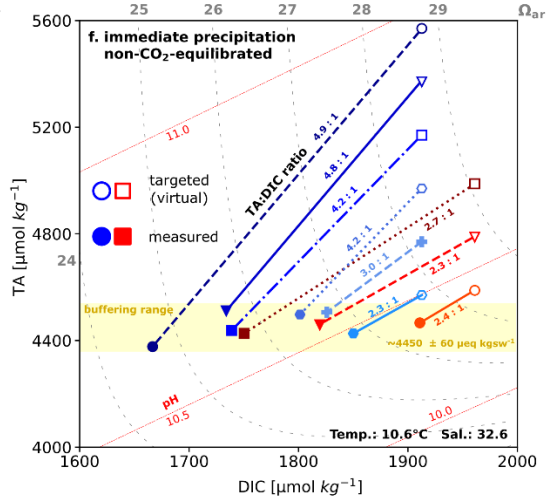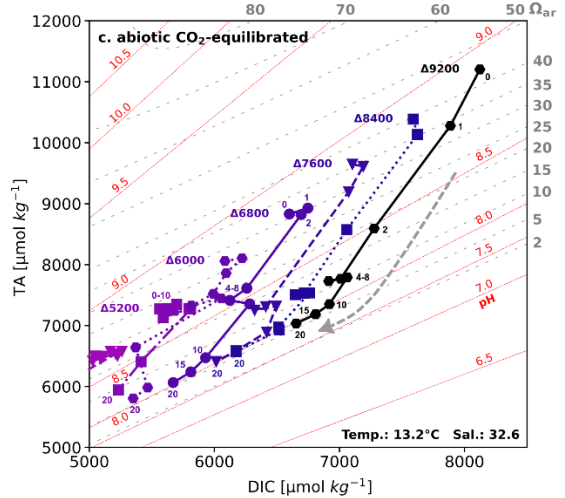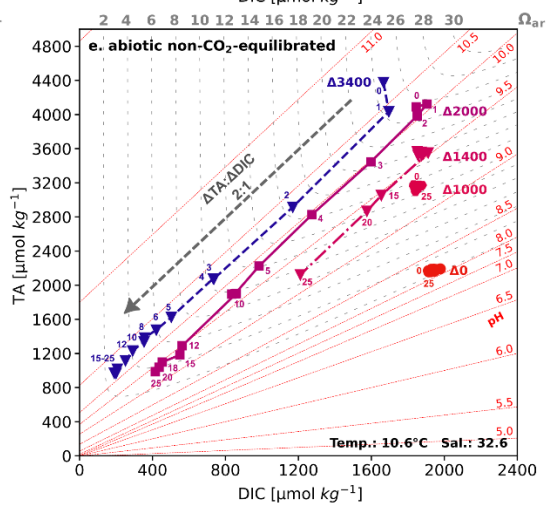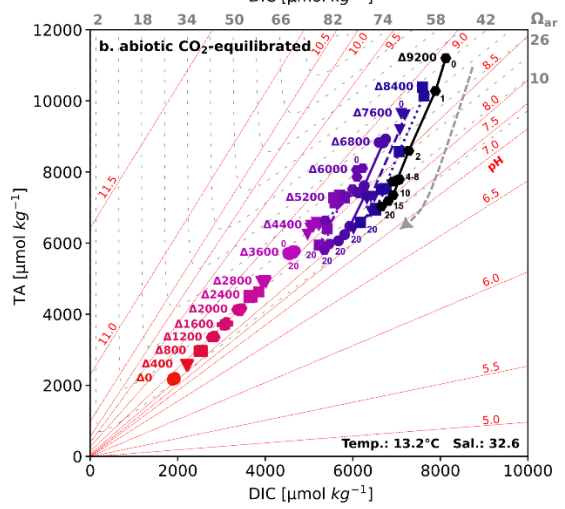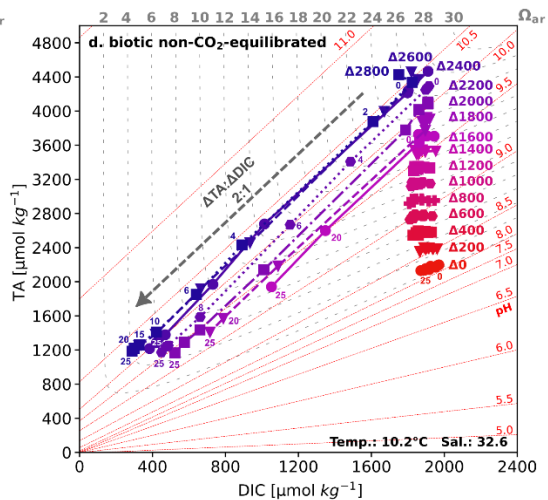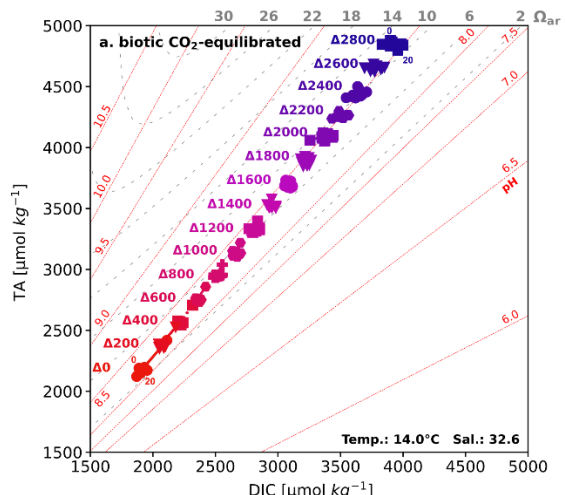Figure 4: TA:DIC diagrams (a.) CO_2-equilibrated (biotic), (b.) CO_2-equilibrated (abiotic), (c.) zoom into precipitating treatments in (b.), (d.) non-CO_2-equilibrated (biotic), (e.) non-CO_2-equilibrated (abiotic), due to the extensive number of data points within the abiotic non-CO_2-equilibrated approach, only selected treatment levels are shown, a complete overview is provided in the supplements (Fig. S4), a selection of data points is labeled with their corresponding sampling day; (f.) comparison of targeted and measured values for treatments with immediate precipitation (blue) abiotic (red) biotic non-CO_2-equilibrated, indicating the formation of a non-carbonate phase like $Mg(OH)_2$; note that due to varying temperatures during the experiments, given the $\Omega_{aragonite}$ and pH contours in all diagrams are temperature and salinity-dependent, potentially resulting in slight inaccuracies in showing exact values for individual data points

3.4 TA loss rates

TA-loss rates for treatments which underwent the precipitation process exhibited similar relationships, independent of the CO_2-equilibration state. In regular patterns, elevated initial TA-levels induced an earlier initiation of the exponential decay process accompanied by increased TA loss rates within each experiment (see Figs. 5 and S9). Absolute rates were dependent on the potential for TA loss within each treatment, regulated by the initial DIC and $\Omega_{aragonite}$ values. Irrespective of the initial TA-level, treatments that showed an immediate precipitation in both non-CO_2-equilibrated experiments exhibited almost identical development trends during the precipitation process. Figure 6 showcases the related temporal TA development of the abiotic CO_2-equilibrated and biotic non-CO_2-equilibrated approaches. Outlier values from a few sampling days were excluded for the calculation of TA loss rates in the abiotic CO_2-equilibrated and abiotic non-CO_2-equilibrated experiments. For details see section "outliers" in the supplements.
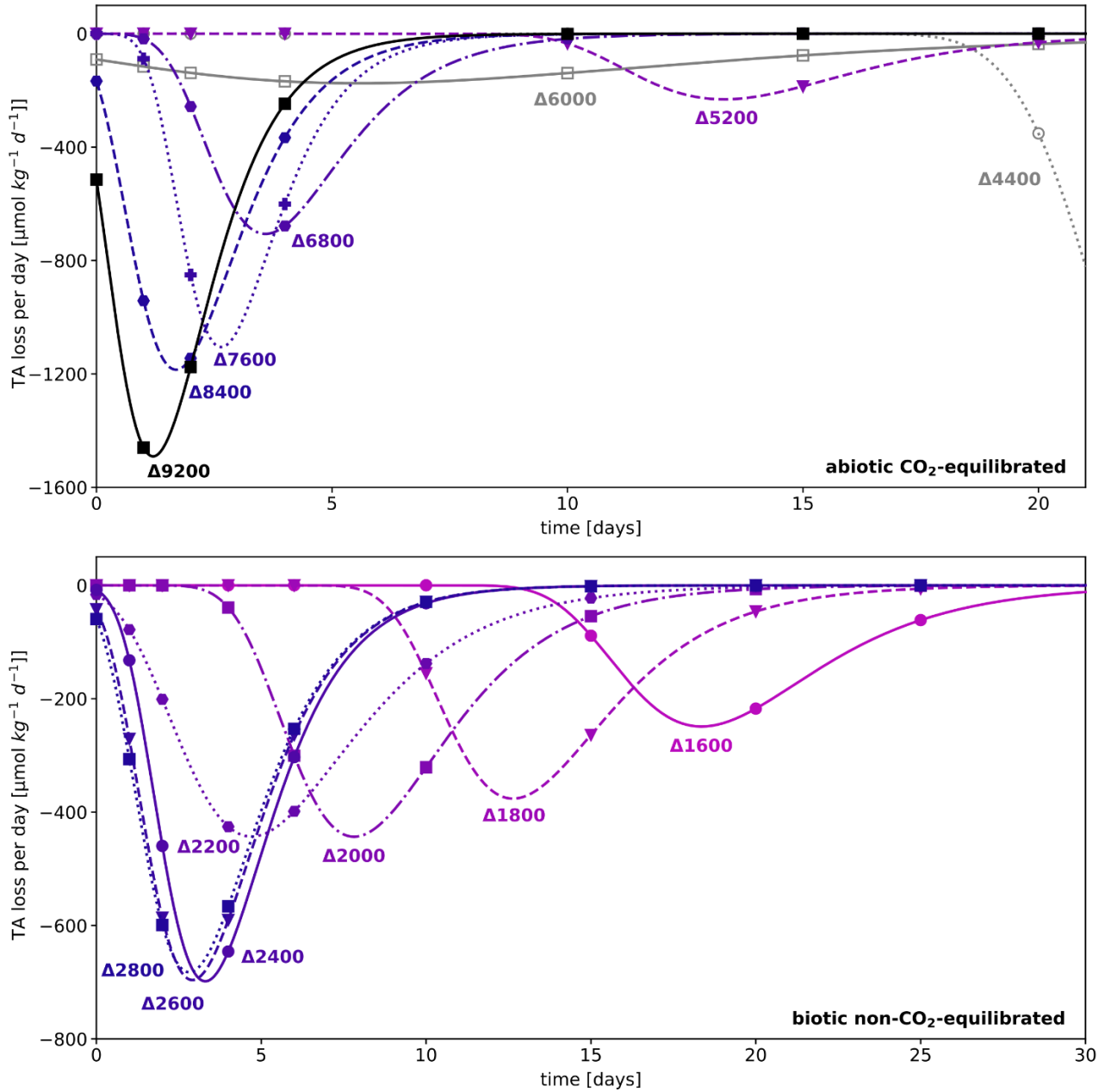
14

Figure 5: TA loss rates per day in (a.) abiotic CO$_2$-equilibrated and (b.) biotic non-CO$_2$-equilibrated experiments showing precipitation processes, rates were calculated based on differentiating functions determined by a sigmoidal curve fit model of the temporal development of TA (see Fig. 6); due to missing data points, rates for treatment levels Δ4400 and Δ6000 in (a.) could not be determined. Regarding ΔTA6000 see description of outliers in the supplements; for TA loss rates of the abiotic non-CO$_2$-equilibrated experiment see Fig. S7
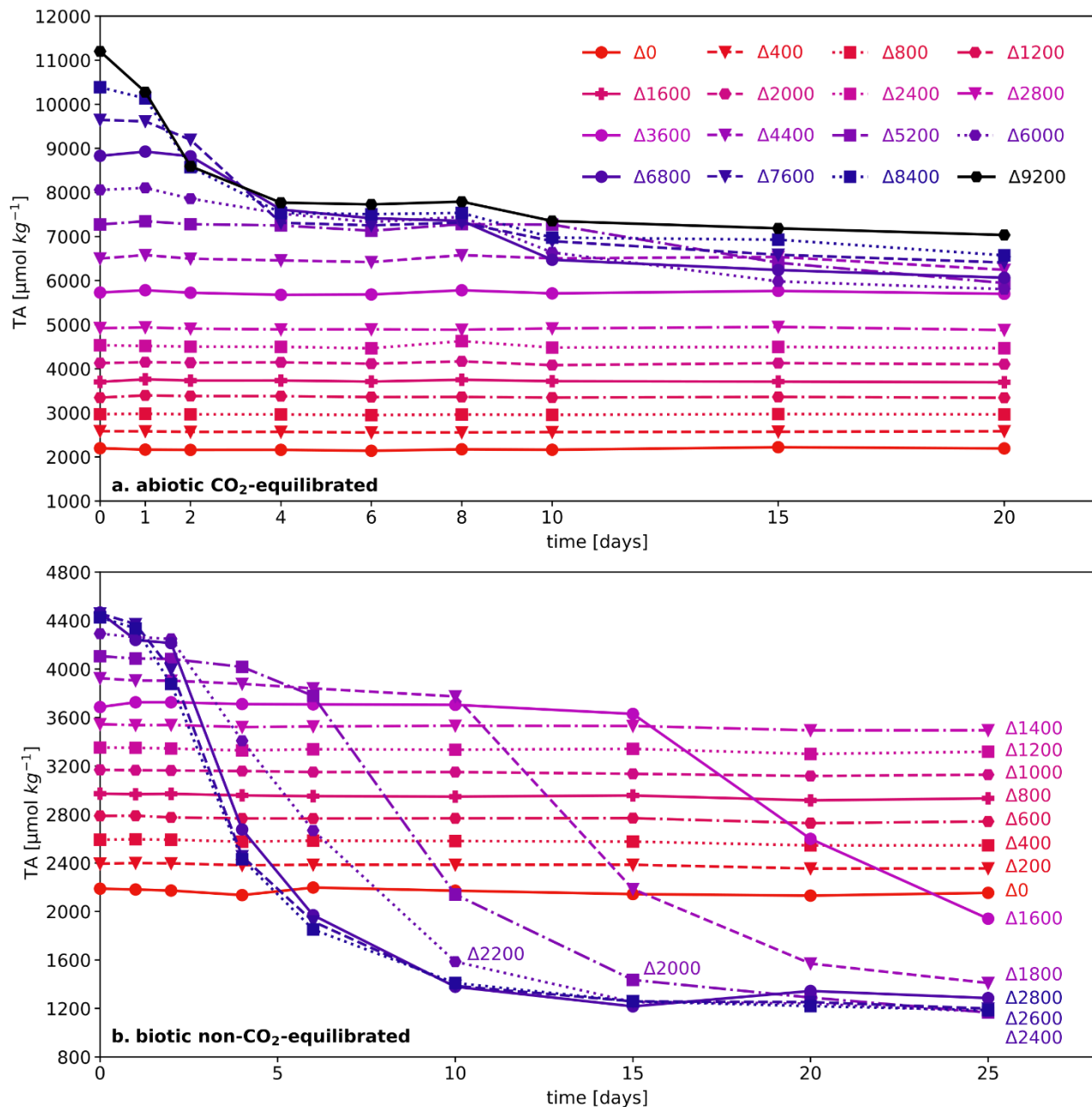
Figure 6: Temporal development of TA in (a.) abiotic CO_2-equilibrated approaches and (b.) biotic non-CO_2-equilibrated experiments; compare to related TA loss rates in Fig. 5, temporal plots for each experiment are provided in the supplements (Fig. S5-8)

3.5 SEM

SEM images of the filtered residua of the experiments show a variety of common shapes of aragonite precipitates. Throughout all conducted experiments in this study visual identifiable precipitates only appeared in treatments which also exhibited a decline in TA. The morphologies of the particles in the CO_2-equilibrated and non-CO_2-equilibrated treatments were identical if secondary mineral formation was triggered. The quantity, structures and shapes of the particles evolved with increased alkalinity. Figure 7 provides examples of different development stages over the runtime of 6 days in the non-CO_2-equilibrated biotic experiment. The bulk of particles showed central stems, which branched out to each end. Morse et al. (2007) described the more developed shapes as "broccoli" structures, due to its physical appearance, while Nielsen et al. (2014) entitled the less branched shapes as "sheaf-of-wheat" bundle. These symmetric particles were the dominant appearing shapes of secondary phases. Treatment levels with initial precipitation showed early stages of stem-like structures with no or very little branching. With higher alkalinity addition more advanced shapes and sizes were predominant, characterized by progressive outbranching. Most developed stages exhibited a merging of the fanned out ends to form closed spheres. Next to the dominant simple stems, multipolar particles, with up to six branches were observed, at all development stages. Despite the variable initial branching numbers, the growth behavior followed the same patterns. Following the scheme presented in Fig. 7 all variants finally reached a closed structure. Observed ellipsoid shaped particles might indicate that the previous precipitate was bi-polar, while more spherical ones had a multi-polar origin. No indications for hollow stems, like described in Hartmann et al. (2023), could be observed. Sizes vary from 2-5 µm for initial shapes, to 10-30 µm for non-closed "broccoli" particles and up to 80 µm for complete spherical forms. For an overview of occurrence and distribution of particle sizes and shapes see Fig. 8(a-f). Consistently higher loss of TA during the runaway process resulted in greater numbers and more developed stages in the precipitates. EDX-analysis uniformly identified the precipitates as Ca-dominated carbonates (Ca: 8.39 ±2.06 mol%, Mg: 4.07 ±0.98 mol%, Na: 0.65 ±0.16 mol%, C: 20.41 ±1.10 mol%, O: 64.8±2.11 mol%, and Cl: 0.47 ±0.05 mol% - median ±half-IQR; Zeiss Gemini Ultra55 Plus (CAU)) with indications of a relatively high content of Mg carbonates phases.
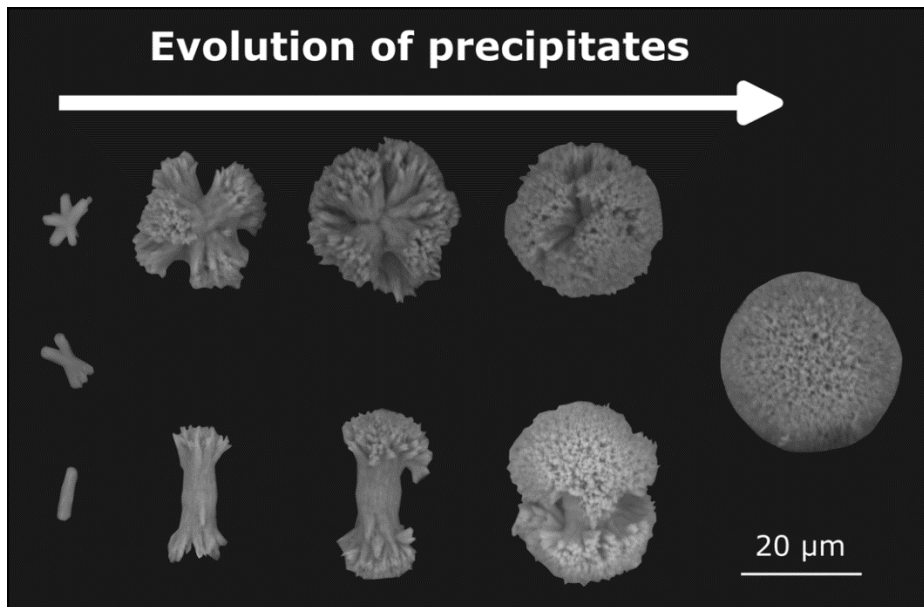
Figure 7: Scheme of the evolution of precipitates, showing a selection of precipitated particles in different development stages. Growth of the initial "stem" structure is accompanied by outbranching on each end. Independent of the polarity of the initial stems, developed particles uniformly form spherical shapes, Tabletop Microscope Hitachi TM4000plus (UHH)
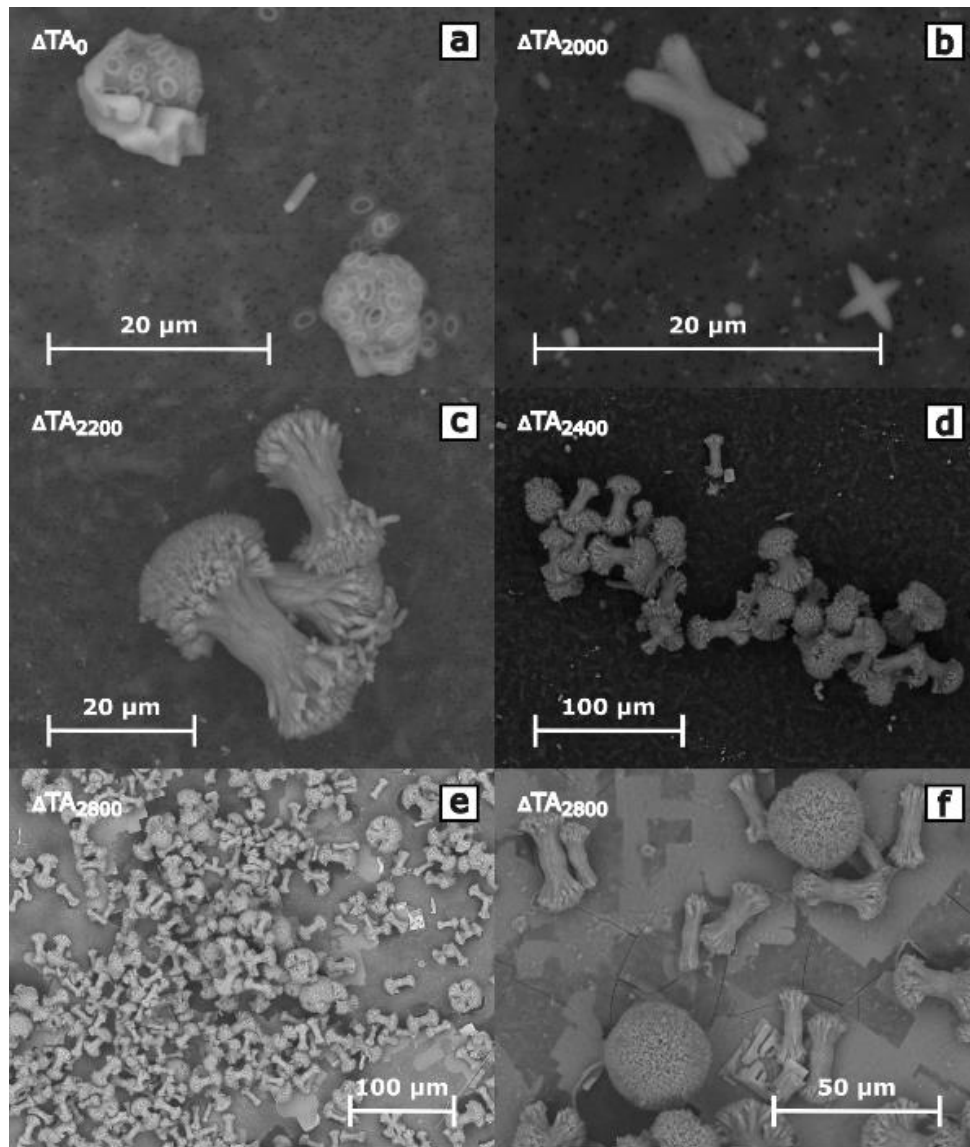
235

Figure 8: SEM images, overview of shapes and occurrences of precipitates in the biotic non-CO_2-equilibrated treatments; no difference could be determined in shapes and appearance within other experiments; compare to Boon et al. (2020), Morse et al. (1997), Pan et al. (2022), Nielsen et al. (2014) and Hartmann et al. (2023), who showed similar shaped carbonate/aragonite precipitates, Tabletop Microscope Hitachi TM4000plus (UHH)

236

4 Discussion

The stability of achieved TA enhancements varied from several hours to weeks, depending primarily on the resulting $\Omega_{aragonite}$, the CO_2-equilibration state, local environmental conditions, and the quantity of introduced alkalinity. While target TA levels were achieved within acceptable tolerances, treatment levels exceeding pH values of approximately 10.3 failed to achieve the intended TA values when measured within three minutes after application. Such observation is potentially the result of immediate magnesium hydroxide formation, buffering the injected alkalinity, as indicated by Eisaman et al. (2023) and Cyronak et al. (2023). While runaway calcium carbonate formation was demonstrated in previous research (Moras et al., 2022; Hartmann et al., 2023), a systematic description of TA loss with respect to time and saturation state could be established here. This allows for the prediction of TA loss behavior when local environmental parameters are well-defined. Consequently, such systematic studies will provide needed parameterized functions for models to assess the consequences of OAE before application (Fennel et al., 2023). Together with addressing the mixing of treated and untreated water, ultimately diluting the additional seawater TA, an assessment of the stability of alkalinity could be generated, if sufficient systematic studies were conducted. Remarkably in the CO_2-equilibrated approach for additions of up to 3600 μmol kg^{-1}, no TA loss was observed within the first 20 days, highlighting the relevance of the equilibration state of the carbonate system for the stability of alkalinity.

4.1 Runaway CaCO₃ precipitation

While the objective of this study was to detect stable alkalinity ranges, exceeding critical limits caused runaway carbonate formation, which leveled out at a new equilibrium. EDX-analysis of the precipitates (see section 3.5) and the 2:1 $\Delta TA:\Delta DIC$ decline ratios (Fig. 4) confirmed the formation of $CaCO_3$ phases when pH-values were below 10.3.

Independent of the CO_2-equilibration state or initial treatment level, the temporal TA development patterns after the start of runaway precipitation could be fitted with a sigmoidal function. Start of runaway precipitation, TA loss rate, and duration of TA decline (Figs. 2-6) varied with temperature and initial TA and DIC treatment levels, but followed a general pattern (see Fig. 9):

    1. Nucleation phase – stage of generation or provision of sufficient surface area to trigger the runaway process

    2. Precipitation phase – stage of exponential decay in TA and DIC in a 2:1 ratio, due to the runaway process, until the potential declines significantly with reduced $\Omega_{aragonite}$ values

    3. New equilibrium - final state after the runaway process ended where the changes in TA and DIC might be too low to be measured
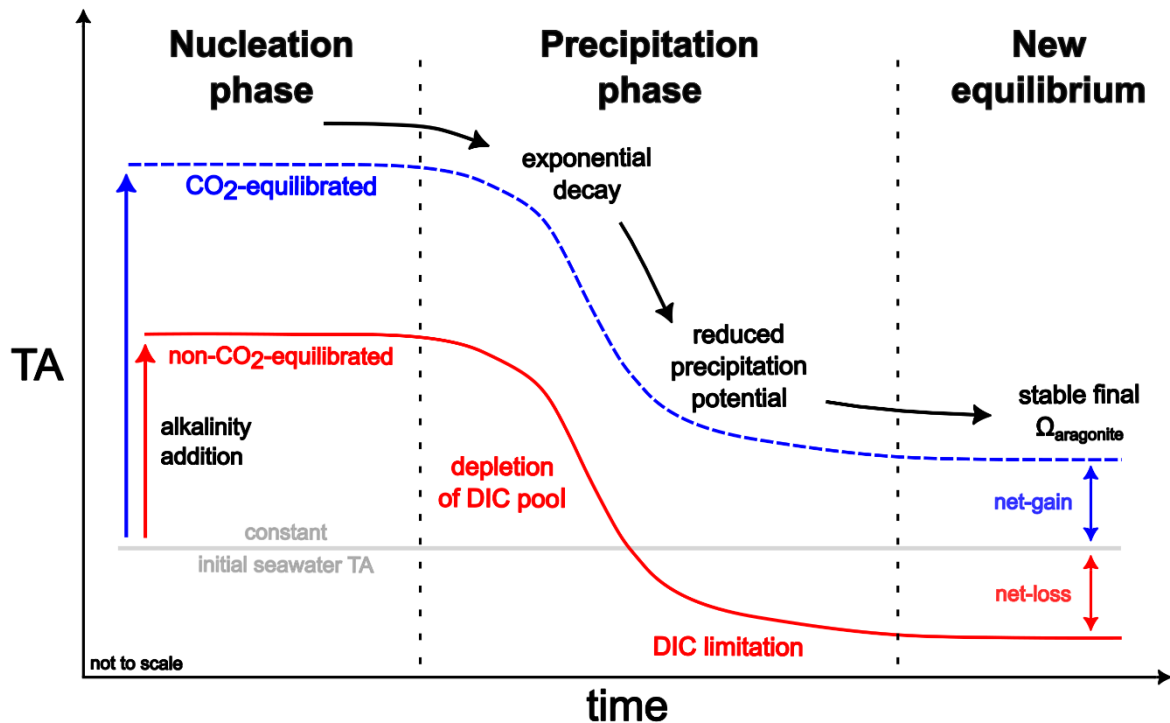
Figure 9: Concept of carbonate runaway precipitation, showing the generalized evolution of TA for non-CO_2-equilibrated and CO_2-equilibrated alkalinity addition scenarios, deduced from experimental results of this study (not to scale). As nucleation is a time dependent process, despite overcritical $\Omega_{aragonite}$ values, a stable temporal state without observable precipitation exists, depending on the physicochemical conditions ranging from seconds to years. While the secondary carbonate formation in the non-CO_2-equilibrated treatments results in TA values below the initial seawater levels, CO_2-equilibrated treatments might, despite a substantial TA loss during the runaway process, achieve a net gain in alkalinity. For further descriptions see text.

267

268 **4.1.1 Nucleation phase**

269 The duration of the nucleation phase varies depending on the quantity and form of added alkalinity, and the alterations in the
270 saturation state, in this work ranging from immediate precipitation to several weeks. However, the nucleation phase might last
271 as long as thousands of years (c.f., Pytkowicz, 1973). To date, only a small amount of data is available to parameterize the
272 duration of this phase systematically. These data are needed for models to assess the consequences of OAE applications (Fennel
273 et al., 2023).
274 Other factors such as temperature or the presence of suitable surfaces for pseudo-homogeneous or heterogeneous precipitation
275 that were not studied here have an influence on the duration of the nucleation phase and have been suggested as triggers for

276   CaCO$_3$ precipitation. These suitable surfaces can include but are not limited to fluvial or marine re-suspended particles
277   (Wurgaft et al., 2021; 2016), seafloor sediments (e.g. CaCO$_3$, quartz particles; Moras et al., 2022), small biotic and abiotic
278   particles (<50 µm) (Hartmann et al., 2023), seagrass, shells, biofilms, and biological activity (Aloisi et al., 2006, Zhu &
279   Dittrich, 2016).

280   Dissolving alkaline particles like Ca(OH)$_2$ or Mg(OH)$_2$ for OAE could also serve as starting points for carbonate formation
281   (Moras et al., 2022; Hartmann et al. 2023). When relying on solid alkaline materials, Moras et al. (2022) and Schulz et al.
282   (2023) suggested that an $\Omega_{aragonite}$ of 5 should not be exceeded, above which CaCO$_3$ runaway precipitation appears to be
283   triggered. However, under the conditions of this study, i.e., with liquid alkaline material, the $\Omega_{aragonite}$ threshold for the initiation
284   of spontaneous pseudo-homogeneous carbonate formation in particle-free seawater is approximately 11.3 at a salinity of 32.6
285   and ~11°C (Marion et al., 2009 – based on data from Morse & He, 1993). Most ocean surface waters are naturally oversaturated
286   with carbonates ($\Omega_{aragonite}$ ~2-5, Olsen et al., 2018), yet no obvious spontaneous inorganic carbonate formation is occurring., as
287   the presence of Mg^{2+} (Berner, 1975; Pan et al., 2021), phosphate (Burton & Walter, 1990), and dissolved organic matter species
288   (Chave & Suess, 1970; Kellock et al., 2022) are known to delay or inhibit precipitation of CaCO$_3$. Since Mg^{2+} in an open ocean
289   context correlates to salinity, its concentration could vary depending on the local conditions (Moras et al., 2023), while
290   phosphate and DOM concentrations are related to biological processes and seasonal changes.

291

292   **4.1.2 Runaway precipitation phase: general patterns**

293   The precipitation phase, characterized by the previously discussed parameters guiding the runaway patterns, might also be
294   influenced by the concentration and quality of formed particles. In contrast to a natural open ocean environment, where
295   precipitates could sink and be removed from the alkalinity-enhanced water, the experimental setup here did not take this into
296   account.

297   It is imperative to investigate if the particle export mechanism could affect the shape of the identified runaway precipitation
298   patterns, e.g. by lower TA loss rates due to less available suitable surface areas for carbonate formation. The experiments in
299   this study were performed in bottles, where the presence of precipitation became evident through a fine whitish coating forming
300   on the inner surface of the water-exposed part of the bottles. Despite being a laboratory artefact, the abundant presence of
301   suspended particles suggests that in the open ocean, similar precipitation patterns could occur. The observation of crystal
302   growth on the bottle walls suggests that the results here and the functional relationships of the runaway precipitation might be
303   impacted by the experimental setup, leading to higher precipitation rates due to increased potential for TA loss. Therefore,
304   field experiments addressing this issue and confirming or improving the parameterization of the loss functions are
305   recommended.

In natural settings, comparable TA decline patterns were observed in river plumes with high degrees of suspended particles (Wurgaft et al., 2021; 2016) or whiting events on the Great Bahama Bank (Broecker & Takahashi, 1966; Morse et al., 2003). One study suggested that with thermohaline stratification and moderate background saturation states in an open water column, TA loss due to carbonate formation may happen because of strong evaporation of water in the eastern Mediterranean Sea (Bialik, 2022). The observation that runaway events could occur naturally under certain constrained conditions highlights the importance of identifying underlying processes before OAE applications are implemented, as the higher saturation states induced by OAE could make such events likelier.

While the fundamental patterns of changes in the carbonate system parameters during the runaway process were dictated by carbonate formation, the starting and ending points of the procedure were dependent on the initial TA/DIC configuration and the resulting $\Omega_{aragonite}$ achieved through manipulation. The observed differences in TA-loss in CO_2-equilibrated and non-CO_2-equilibrated approaches were therefore expected. Under well-defined circumstances and aware of a practical final $\Omega_{aragonite}$ saturation state range, the consequences of a completed runaway precipitation process should, in theory, therefore be predictable.

As shown in Figures 2-4, treatments which underwent a runaway process approached relatively uniform final $\Omega_{aragonite}$ values, indicating that Ω-values served as the decisive factor in delineating the termination of the runaway precipitation process. Including results from this work, runaway precipitation processes in natural or artificial seawater in comparable studies (Moras et al, 2022; Hartmann et al., 2023; Fuhr et al., 2022; Pan et al., 2021) approached final $\Omega_{aragonite}$ values between 1.5 and 5.0. The variations in the final $\Omega_{aragonite}$ across the different approaches could be attributed to differences in framework conditions such as temperature, salinity, CO_2-equilibration state, agitation methods or sediment concentration during the course of the experiments.

4.1.3 CO₂-equilibration states

While the precipitation rates in this study decreased significantly at the end of each experiment, approaching $\Omega_{aragonite}$ values of 2.5-5.0, it cannot be excluded that further formation of secondary phases could have continued. While some treatments within the non-CO_2-equilibrated experiments still experienced a daily decline of 1-10 $\mu mol\ kg^{-1}$ in TA during the last 5 days of operation, these changes were relatively insignificant compared to their earlier rates. Nonetheless, slight changes were still observed, and it cannot be ruled out that the process stopped after a runtime of 25 days.

In contrast to the non-CO_2-equilibrated approach, the CO_2-equilibrated experiments showed relatively constant final $\Omega_{aragonite}$ values of 5.8-6.0 at the end of the abiotic experiments after 20 days. The runaway process is anticipated to persist at lower levels of TA loss rates, given that they consistently declined by 20-30 $\mu mol\ kg^{-1}$ per day during the final 5 days of operation.

4.1.4 Comparison to other experiments

Time spans to reach the end of the runaway precipitation process in studies with comparable setups, solely focusing on non-CO_2-equilibrated treatments with a ΔTA_{added} of 2000 µmol kg^{-1}, ranged from 4 days in Hartmann et al. (2023) to more than 14 days in Moras et al. (2022). In Moras et al. (2022), there were variations in the experimental conditions, such as the use of solid $Ca(OH)_2$ for TA-enhancement, constant agitation, and a temperature of 21°C. These differences may hinder a direct comparison with our study. By contrast, this study employed the configuration introduced by Hartmann et al. (2023), with the only distinction being the utilization of seawater with a salinity of 36.2 and a temperature of around 23°C. In this study, with a salinity of 32.6 and temperatures ranging from 10 to 16°C, the precipitation process in the highest treatments came close to a halt after ~15 days in the non-CO_2-equilibrated approaches, while alkalinity was stable over 20 days in CO_2-equilibrated treatments with ΔTA_{added} up to 3600 µmol kg^{-1}. However, in Hartmann et al. (2023) experiments, significantly faster precipitation rates were observed. This underscores the crucial influence of local environmental factors and application scenario in shaping the dynamics of the runaway process.

Following the Ω-threshold described by Marion et al. (2009), experimental results from Pytkowicz (1973) and considering the general trend predictions from the TA-loss rates (Fig. 5), it is suggested that further treatments in this study might have initiated the runaway process if the experiments had continued. Therefore, treatment levels above $\Delta TA600$ µmol kg^{-1} in the non-CO_2-equilibrated and $\Delta TA2400$ µmol kg^{-1} in CO_2-equilibrated approaches had the potential to start carbonate precipitation.

As manipulated water parcels in real world application scenarios would be diluted by untreated water, the results of our study suggest a functional relationship with time for the dilution of TA-enhanced water to non-critical $\Omega_{aragonite}$ values. This could range from minutes to weeks (e.g. see Figs. 4 and 10), dependent on the local physicochemical conditions, the CO_2-equilibration state, and the achieved TA levels. Further research is therefore needed to identify the functional relationship for other environmental settings such as temperature, salinity, and the impact of particles for near coastal settings. This is necessary to determine if the here identified relationships are universally valid, or in the context of OAE, further factors need to be considered. In addition, experiments on the dilution of manipulated water masses are needed to test whether TA values exceeding critical ranges can be stabilized. By understanding patterns and factors driving the runaway process, measures could be taken to prevent unwanted consequences during TA addition.

4.2 Temporal stability after TA addition

In the context of an open ocean application of OAE, induced turbulence and advective energy in the water would cause the mixing of the alkalized water body with untreated surrounding seawater. Specifically, ship-based applications offer the potential to significantly change the concentrations and saturation states in a relatively short amount of time (e.g. Caserini et al., 2021; He & Tyka, 2023; Renforth & Henderson, 2017). Dilution could potentially prevent or delay the nucleation phase for a significant amount of time, to a degree that runaway precipitation events can be avoided at time scales relevant for CDR.

While TA values reached in this study might not represent final targeted TA levels for a real-world application after immediate dilution with untreated water parcels, studied ranges provide experimental insight into processes during transient enhanced conditions, occurring around point sources or in (partially-) enclosed water bodies without adequate mixing. Derived from the results of non-CO_2-equilibrated setups, Fig. 10 provides an overview of TA ranges and timeframes until a manipulated water mass should be diluted to prevent the onset of secondary mineral formation. Note that for the CO_2-equilibrated approaches, this study could not determine reliable comparable stability ranges.
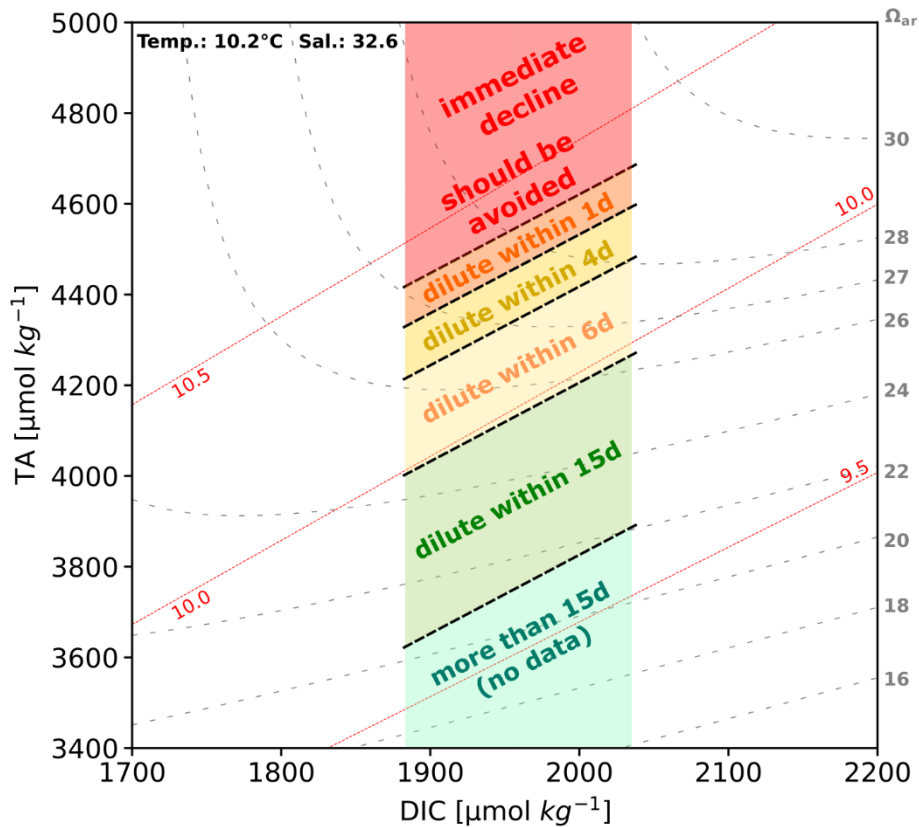

Figure 10: Stability ranges during non-CO_2-equilibrated experiments showing upper critical limits for application, which should be avoided to prevent runaway precipitation and its consequences. ΔTA0 (TA: ~2200 μmol kg^{-1}, DIC ~ 1960 μmol kg^{-1}, pH ~8.2, temperature 10.2°C, salinity 32.6), the red area highlights the critical zone for immediate precipitation, tolerance in time for dilution or other actions to prevent the runaway process are indicated. Ranges in this diagram are applicable only to this setting and should not be generalized.

As described above, treatments which reached TA-levels above 4450 μmol kg^{-1} within the non-CO_2-equilibrated approach immediately lost parts of the added TA. To avoid any kind of secondary mineral formation under the local conditions of the Raunefjord, these values should not be surpassed without additional measures. In theory, every ocean water mass should possess such a critical threshold level for immediate precipitation. This threshold would determine the practical upper limit for the application scenarios and overall efficiency of OAE. At present, there does not seem to be a comprehensive method for calculating this upper threshold. Such a method would need to take into consideration the complexities of the natural environment such as seasonal and biological cycles, distinct geographical characteristics, and the various approaches of TA addition. To derive such a method would need systematic research to identify relevant factors and field trials aimed at exploring their interactions under real-world conditions. Nevertheless, results of this study also showed that TA could be enhanced above ΔTA_{added} of 2000 μmol kg^{-1} in a non-CO_2-equilibrated style without any adverse geochemical consequences if sufficient mixing is ensured within the given local temporal stability ranges.

4.3 Immediate magnesium hydroxide precipitation

If by addition of NaOH to seawater a pH of 10.4 (at 21 °C) is reached, $Mg(OH)_2$ is formed. This is a long-known process as described by Haas (1916) and Kapp (1928) and comparable to values reached in this study within the non-CO_2-equilibrated treatments, showing an immediate TA decline (pH 10.3-10.6, at 10-12°C). This suggests that the aforementioned process could potentially account for the immediate precipitation observed in the present experiments. As described by Turek & Gnot (1995), the formation of $Mg(OH)_2$ during this practice could be considered as an "immediate process", which aligns with observations in this study. The buffering of TA by $Mg(OH)_2$ formation during TA injection was also supported by the ΔTA: ΔDIC change ratios of 2.3-4.9:1 (Fig. 4f) immediately after alkalinity addition. Co-precipitation of carbonate phases besides the generation of $Mg(OH)_2$ would be necessary to achieve these change ratios and is a regular feature in seawater (Battaglia et al., 2022; Nguyen Dang et al., 2017; Turek & Gnot, 1995). Formed solid $Mg(OH)_2$ particles could have acted as triggers for further precipitation of carbonate phases and leading to the observed earlier initiation of the runaway process.

During the injection of NaOH stock solution in seawater, the sharp gradient in pH/TA concentrations could lead to the generation of lysospheres and floccules, which aggregate and enclose water in its pore space (Turek & Gnot, 1995). Similar observations were made by Badjatya et al. (2022), who described it as colloidal suspension. While the addition levels were significantly lower in this study as compared to Badjatya et al. (2022), a comparable trend after the injection was evident. This trend was visually observable across all non-CO_2-equilibrated treatments above $\Delta TA200$. However, to observe the same phenomenon in the CO_2-equilibrated approaches, higher treatment levels ($>\Delta TA2000$) were required to form aggregates.

In the absence of further agitation, aggregates that had formed remained visible for several days. However, when the bottles were gently rotated after the TA addition, aggregates disintegrated and all treatments that were initially below the critical threshold for immediate precipitation reached their target TA levels. These observations suggest that the immediate formation

405   of potential $Mg(OH)_2$ aggregates during the injection process might be reversible, as also noted by Cyronak et al. (2023). In a

406   real world scenario, wave movement and dilution processes with untreated waters might allow the redissolution of $Mg(OH)_2$

407   or further metastable carbonate phases.

408   Effects like an increase in undesired turbidity during TA addition as stated by Eisaman et al. (2023) might therefore be

409   temporal. Depending on the speed of the redissolution process, sedimentation of the aggregates might function as an export

410   factor, transferring the added alkalinity to greater depths. The enclosed water in the lysospheres might nevertheless reduce the

411   sinking rate significantly due to its relatively low density (Turek & Gnot, 1995).

5 Conclusion

After the introduction of the runaway precipitation concept by Moras et al. (2022) and Hartmann et al. (2023), this study has identified functional relationships of TA change rates after initiation of the secondary carbonate formation process. With well-defined framework parameters of $\Omega_{aragonite}$, temperature, and salinity, it is therefore possible to predict the temporal evolution of alkalinity. Once the runaway process was triggered, patterns of TA loss were identical for both CO_2-equilibrated and non-CO_2-equilibrated TA addition approaches. While a progressing runaway process negatively impacts carbonate chemistry parameters, the observed delayed onset of detectable solid phase formation implies that alkalinity could be enhanced beyond 2000 μmol kg^{-1}, when sufficient dilution with untreated water could be ensured within given time ranges. With knowledge of the local environmental conditions, introduced $\Omega_{aragonite}$, and CO_2-equilibration state, it is hypothesized that it is possible to predict a temporary stability range for any given system. The ability to predict the outcomes in advance can facilitate environmental assessments prior to OAE applications. Furthermore, the parameters acquired could be essential for computer models to carry out these evaluations.

The seawater used in this study had low sediment concentrations, therefore identified TA rate changes during runaway precipitation or temporary stability ranges might differ for systems with higher suspended sediment concentrations, especially if suitable crystal surfaces are abundant (c.f. Moras et al., 2022; Hartmann et al., 2023). Unlike in Hartmann et al. (2023), no relevant differences between biotic and abiotic approaches (distinguished by the filter mesh size) could be identified.

For non-CO_2-equilibrated TA additions, an upper pH threshold of around 10.3 could be observed. Crossing this threshold comes with the potential consequence of magnesium hydroxide formation, which was also seen in other studies (c.f. Badjatya et al., 2022; Turek & Gnot, 1995; Vassallo et al., 2021). Considerations about the TA-treatment levels in open ocean application scenarios must therefore consider the onset of $Mg(OH)_2$ formation as an upper threshold. To maximize effectiveness, it is crucial to maintain concentrations just below this critical value when injecting alkalinity into seawater, especially if the local seawater possess efficient dilution capabilities.

These considerations are relevant for modelling the limitations and dynamics of alkalinity enhancement in the ocean, as demonstrated by He and Tyka (2023). Nevertheless, it is essential to validate these findings with in situ experiments to establish parameters and functional relationships applicable to open ocean environments. It is only under these circumstances that accurate assessments can be made. The most promising outcome of this study is the possibility to predict abiotic processes and the stability of alkalinity for effective and realistic applications in the future.

Author contributions

The idea for this work was conceived by NS and JH. NS, GF, and CL designed the experiments with help from JH, JS, and UR. NS, CL, GF, and JS carried out sampling and laboratory analysis. NS interpreted the data with help from GF and JH. NS and JH wrote the text with contributions from all co-authors.

Acknowledgements

Financial support

Competing interests

JHA is a co-founder of the Planeteers GmbH. The contact author has declared that all other authors have no competing interests.

References

Albright, R., Caldeira, L., Hosfelt, J., Kwiatkowski, L., Maclaren, J. K., Mason, B. M., Nebuchina, Y., Ninokawa, A., Pongratz, J., Ricke, K. L., Rivlin, T., Schneider, K., Sesboüé, M., Shamberger, K., Silverman, J., Wolfe, K., Zhu, K., and Caldeira, K.: Reversal of ocean acidification enhances net coral reef calcification, Nature, 531, 362–365, https://doi.org/10.1038/nature17155, 2016.

Aloisi, G., Gloter, A., Krüger, M., Wallmann, K., Guyot, F., and Zuddas, P.: Nucleation of calcium carbonate on bacterial nanoglobules, Geology, 34, https://doi.org/10.1130/g22986a.1, 2006.

Bach, L. T., Gill, S. J., Rickaby, R. E. M., Gore, S., and Renforth, P.: CO2 Removal With Enhanced Weathering and Ocean Alkalinity Enhancement: Potential Risks and Co-benefits for Marine Pelagic Ecosystems, Frontiers in Climate, 1, 1038, https://doi.org/10.3389/fclim.2019.00007, 2019.

Badjatya, P., Akca, A. H., Fraga Alvarez, D. V., Chang, B., Ma, S., Pang, X., Wang, E., van Hinsberg, Q., Esposito, D. V., and Kawashima, S.: Carbon-negative cement manufacturing from seawater-derived magnesium feedstocks, Proc Natl Acad Sci U S A, 119, e2114680119, https://doi.org/10.1073/pnas.2114680119, 2022.

Badocco, D., Pedrini, F., Pastore, A., di Marco, V., Marin, M. G., Bogialli, S., Roverso, M., and Pastore, P.: Use of a simple empirical model for the accurate conversion of the seawater pH value measured with NIST calibration into seawater pH scales, Talanta, 225, 122051, https://doi.org/10.1016/j.talanta.2020.122051, 2021.

Battaglia, G., Domina, M. A., Lo Brutto, R., Lopez Rodriguez, J., Fernandez de Labastida, M., Cortina, J. L., Pettignano, A., Cipollina, A., Tamburini, A., and Micale, G.: Evaluation of the Purity of Magnesium Hydroxide Recovered from Saltwork Bitterns, Water, 15, https://doi.org/10.3390/w15010029, 2022.

Berner, R. A.: The role of magnesium in the crystal growth of calcite and aragonite from sea water, Geochimica et Cosmochimica Acta, 39, 489-504, https://doi.org/10.1016/0016-7037(75)90102-7, 1975.

Berner, R. A., Lasaga, A. C., and Garrels, R. M.: Carbonate-silicate geochemical cycle and its effect on atmospheric carbon dioxide over the past 100 million years, Am. J. Sci.;(United States), 283, https://doi.org/10.2475/ajs.283.7.641, 1983.

Bialik, O. M., Sisma-Ventura, G., Vogt-Vincent, N., Silverman, J., and Katz, T.: Role of oceanic abiotic carbonate precipitation in future atmospheric CO(2) regulation, Sci Rep, 12, 15970, https://doi.org/10.1038/s41598-022-20446-7, 2022.

Boon, M., Rickard, W. D. A., Rohl, A. L., and Jones, F.: Stabilization of Aragonite: Role of Mg2+ and Other Impurity Ions, Crystal Growth & Design, 20, 5006-5017, https://doi.org/10.1021/acs.cgd.0c00152, 2020.

Broecker, W. S. and Takahashi, T.: Calcium carbonate precipitation on the Bahama Banks, Journal of Geophysical Research, 71, 1575-1602, https://doi.org/10.1029/JZ071i006p01575, 1966.

Burton, E. A. and Walter, L. M.: The role of pH in phosphate inhibition of calcite and aragonite precipitation rates in seawater, Geochimica et Cosmochimica Acta, 54, 797-808, https://doi.org/10.1016/0016-7037(90)90374-T, 1990.

496 Caldeira, K. and Rau, G. H.: Accelerating carbonate dissolution to sequester carbon dioxide in the ocean: Geochemical
497   implications, Geophysical Research Letters, 27, 225-228, https://doi.org/10.1029/1999gl002364, 2000.

498 Caserini, S., Pagano, D., Campo, F., Abbà, A., De Marco, S., Righi, D., Renforth, P., and Grosso, M.: Potential of Maritime
499   Transport for Ocean Liming and Atmospheric CO2 Removal, Frontiers in Climate, 3,
500   https://doi.org/10.3389/fclim.2021.575900, 2021.

501 Chave, K. E. and Suess, E.: Calcium Carbonate Saturation in Seawater: Effects of Dissolved Organic Matter, Limnology and
502   Oceanography, 15, 633-637, https://doi.org/10.4319/lo.1970.15.4.0633, 1970.

503 Cyronak, T., Albright, R., and Bach, L.: Chapter 4.5: Field Experiments, State of the Planet Discussions, 2023, 1-25,
504   https://doi.org/10.5194/sp-2023-9, 2023.

505 Deffeyes, K. S.: Carbonate Equilibria: A Graphic and Algebraic Approach1, Limnology and Oceanography, 10, 412-426,
506   https://doi.org/10.4319/lo.1965.10.3.0412, 1965.

507 Dickson, A. G.: Standard potential of the reaction: AgCl (s)+ 12H2 (g)= Ag (s)+ HCl (aq), and and the standard acidity constant
508   of the ion HSO_4^- in synthetic sea water from 273.15 to 318.15 K, The Journal of Chemical Thermodynamics, 22,
509   113-127, https://doi.org/10.1016/0021-9614(90)90074-Z, 1990.

510 Eisaman, M., Geilert, S., Renforth, P., Bastianini, L., Campbell, J., Dale, A., Foteinis, S., Grasse, P., Hawrot, O., and Löscher,
511   C.: Chapter 3: Assessing the technical aspects of OAE approaches, State of the Planet Discussions, 2023, 1-52,
512   https://doi.org/10.5194/sp-2-oae2023-3-2023, 2023.

513 Fennel, K., Long, M. C., Algar, C., Carter, B., Keller, D., Laurent, A., Mattern, J. P., Musgrave, R., Oschlies, A., and Ostiguy,
514   J.: Modeling considerations for research on Ocean Alkalinity Enhancement (OAE), State of the Planet Discussions,
515   2023, 1-47, https://doi.org/10.5194/sp-2-oae2023-9-2023, 2023.

516 Ferderer, A., Chase, Z., Kennedy, F., Schulz, K. G., and Bach, L. T.: Assessing the influence of ocean alkalinity enhancement
517   on a coastal phytoplankton community, Biogeosciences, 19, 5375-5399, 10.5194/bg-19-5375-2022, 2022.

518 Forster, M.: Investigations for the environmentally friendly production of Na2CO3 and HCl from exhaust CO2, NaCl and
519   H2O, Journal of Cleaner Production, 23, 195-208, https://doi.org/10.1016/j.jclepro.2011.10.012, 2012.

520 Forster, M.: Investigations to convert CO2, NaCl and H2O into Na2CO3 and HCl by thermal solar energy with high solar
521   efficiency, Journal of CO2 Utilization, 7, 11-18, https://doi.org/10.1016/j.jcou.2014.06.001, 2014.

522 Fuhr, M., Geilert, S., Schmidt, M., Liebetrau, V., Vogt, C., Ledwig, B., and Wallmann, K.: Kinetics of Olivine Weathering in
523   Seawater: An Experimental Study, Frontiers in Climate, 4, https://doi.org/10.3389/fclim.2022.831587, 2022.

524 Haas, A. R.: The Effect of the Addition of Alkali to Sea Water Upon the Hydrogen Ion Concentration, Journal of Biological
525   Chemistry, 26, 515-517, https://doi.org/10.1016/s0021-9258(18)87433-6, 1916.

526 Hartmann, J., West, A. J., Renforth, P., Köhler, P., De La Rocha, C. L., Wolf-Gladrow, D. A., Dürr, H. H., and Scheffran, J.:
527   Enhanced chemical weathering as a geoengineering strategy to reduce atmospheric carbon dioxide, supply nutrients,
528   and mitigate ocean acidification, Reviews of Geophysics, 51, 113-149, https://doi.org/10.1002/rog.20004, 2013.

Hartmann, J., Suitner, N., Lim, C., Schneider, J., Marín-Samper, L., Arístegui, J., Renforth, P., Taucher, J., and Riebesell, U.: Stability of alkalinity in ocean alkalinity enhancement (OAE) approaches – consequences for durability of CO2 storage, Biogeosciences, 20, 781-802, https://doi.org/10.5194/bg-20-781-2023, 2023.

He, J. and Tyka, M. D.: Limits and CO2 equilibration of near-coast alkalinity enhancement, Biogeosciences, 20, 27-43, https://doi.org/10.5194/bg-20-27-2023, 2023.

Ilyina, T., Six, K. D., Segschneider, J., Maier-Reimer, E., Li, H., and Núñez-Riboni, I.: Global ocean biogeochemistry model HAMOCC: Model architecture and performance as component of the MPI-Earth system model in different CMIP5 experimental realizations, Journal of Advances in Modeling Earth Systems, 5, 287–315, https://doi.org/10.1029/2012ms000178, 2013.

Kapp, E. M.: The precipitation of calcium and magnesium from sea water by sodium hydroxide, The Biological Bulletin, 55, 453-458, 1928.

Kellock, C., Castillo Alvarez, M. C., Finch, A., Penkman, K., Kroger, R., Clog, M., and Allison, N.: Optimising a method for aragonite precipitation in simulated biogenic calcification media, PLoS One, 17, e0278627, https://doi.org/10.1371/journal.pone.0278627, 2022.

Kheshgi, H. S.: Sequestering atmospheric carbon dioxide by increasing ocean alkalinity, Energy, 20(9), 915-922., https://doi.org/10.1016/0360-5442(95)00035-F 1995.

Koch, C. and Manzur, K.: A new technology of pit lake treatment using calcium oxide and carbon dioxide to increase alkalinity, IMWA 2016 – Mining Meets Water – Conflicts and Solutions, International Mine Water Association, 284–229, 2016.

Köhler, P., Hartmann, J., and Wolf-Gladow, D. A.: Geoengineering potential of artificially enhanced silicate weathering of olivine, Proc Natl Acad Sci U S A, 107, 20228-20233, https://doi.org/10.1073/pnas.1000545107, 2010.

Lee, K., Kim, T.-W., Byrne, R. H., Millero, F. J., Feely, R. A., and Liu, Y.-M.: The universal ratio of boron to chlorinity for the North Pacific and North Atlantic oceans, Geochimica et Cosmochimica Acta, 74, 1801-1811, https://doi.org/10.1016/j.gca.2009.12.027, 2010.

LMBV: In-lake Neutralization of East German Lignite Pit Lakes: Technical History and New Approaches from LMBV, 2017.

Lueker, T. J., Dickson, A. G., and Keeling, C. D.: Ocean pCO2 calculated from dissolved inorganic carbon, alkalinity, and equations for K1 and K2: validation based on laboratory measurements of CO2 in gas and seawater at equilibrium, Marine chemistry, 70(1-3), 105-119, https://doi.org/10.1016/S0304-4203(00)00022-0, 2000.

Mackenzie, F. T. and Garrels, R. M.: Chemical mass balance between rivers and oceans, American Journal of Science, 264, 507-525, https://doi.org/10.2475/ajs.264.7.507, 1966.

Marion, G., Millero, F., and Feistel, R.: Precipitation of solid phase calcium carbonates and their effect on application of seawater S A–T–P models, Ocean science, 5, 285-291, https://doi.org/10.5194/os-5-285-2009, 2009.

Meinshausen, M., Meinshausen, N., Hare, W., Raper, S. C., Frieler, K., Knutti, R., Frame, D. J., and Allen, M. R.: Greenhouse-gas emission targets for limiting global warming to 2 degrees C, Nature, 458, 1158-1162, https://doi.org/10.1038/nature08017, 2009.

Moras, C., Bach, L., Cyronak, T., Joannes-Boyau, R., and Schulz, K.: Effects of grain size and seawater salinity on brucite dissolution and secondary calcium carbonate precipitation kinetics: implications for Ocean Alkalinity Enhancement, Copernicus Meetings, https://doi.org/10.5194/egusphere-egu23-330, 2023.

Moras, C. A., Bach, L. T., Cyronak, T., Joannes-Boyau, R., and Schulz, K. G.: Ocean alkalinity enhancement – avoiding runaway CaCO3 precipitation during quick and hydrated lime dissolution, Biogeosciences, 19, 3537-3557, https://doi.org/10.5194/bg-19-3537-2022, 2022.

Morse, J. W. and He, S.: Influences of T, S and PCO2 on the pseudo-homogeneous precipitation of CaCO3 from seawater: implications for whiting formation, Marine Chemistry, 41(4), 291-297., https://doi.org/10.1016/0304-4203(93)90261-L, 1993.

Morse, J. W., Arvidson, R. S., and Lüttge, A.: Calcium carbonate formation and dissolution, Chemical reviews, 107, 342-381, https://doi.org/10.1021/cr050358j, 2007.

Morse, J. W., Gledhill, D. K., and Millero, F. J.: Caco3 precipitation kinetics in waters from the great Bahama bank, Geochimica et Cosmochimica Acta, 67, 2819-2826, https://doi.org/10.1016/s0016-7037(03)00103-0, 2003.

Morse, J. W., Wang, Q., and Tsio, M. Y.: Influences of temperature and Mg: Ca ratio on CaCO3 precipitates from seawater, Geology, 25, 85-87, https://doi.org/10.1130/0091-7613(1997)025<0085:IOTAMC>2.3.CO;2, 1997.

NASEM: A Research Strategy for Ocean-based Carbon Dioxide Removal and Sequestration, National Academies of Sciences, Engineering, and Medicine, Washington (DC), https://doi.org/10.17226/26278, 2022.

Nguyen Dang, D., Gascoin, S., Zanibellato, A., G. Da Silva, C., Lemoine, M., Riffault, B., Sabot, R., Jeannin, M., Chateigner, D., and Gil, O.: Role of brucite dissolution in calcium carbonate precipitation from artificial and natural seawaters, Crystal Growth & Design, 17, 1502-1513, https://doi.org/10.1021/acs.cgd.6b01305, 2017.

Nielsen, M. H., Aloni, S., and De Yoreo, J. J.: In situ TEM imaging of CaCO(3) nucleation reveals coexistence of direct and indirect pathways, Science, 345, 1158-1162, https://doi.org/10.1126/science.1254051, 2014.

Olsen, A., Lange, N., Key, R. M., Tanhua, T., Álvarez, M., Becker, S., Bittig, H. C., Carter, B. R., Cotrim da Cunha, L., and Feely, R. A.: GLODAPv2. 2019–an update of GLODAPv2, Earth System Science Data, 11, 1437-1461, https://doi.org/10.5194/essd-11-1437-2019, 2019.

Orr, J. C., Epitalon, J.-M., Dickson, A. G., and Gattuso, J.-P.: Routine uncertainty propagation for the marine carbon dioxide system, Marine Chemistry, 207, 84-107, https://doi.org/10.1016/j.marchem.2018.10.006, 2018.

Oschlies, A., Bach, L. T., Rickaby, R. E. M., Satterfield, T., Webb, R., & Gattuso, J.-P. (2023). Climate targets, carbon dioxide removal, and the potential role of ocean alkalinity enhancement. State of the Planet, 2-oae2023, 1-9. https://doi.org/10.5194/sp-2-oae2023-1-2023

Pan, Y., Li, Y., Ma, Q., He, H., Wang, S., Sun, Z., Cai, W.-J., Dong, B., Di, Y., Fu, W., and Chen, C.-T. A.: The role of Mg2+ in inhibiting CaCO3 precipitation from seawater, Marine Chemistry, 237, https://doi.org/10.1016/j.marchem.2021.104036, 2021.

Paul, A., Haunost, M., Goldenberg, S., Sanchez Smith, N., and Riebesell, U.: Testing the response of natural plankton community to ocean alkalinity enhancement in the subtropical North Atlantic Ocean, https://doi.org/10.5194/egusphere-egu23-9528, 2023.

Pierrot, D., Lewis, E., and Wallace, D. W. R.: MS Excel Program Developed for CO2 System Calculations ORNL/CDIAC-105a (Co2sys_v2.5) [code], 10.3334/CDIAC/otg.CO2SYS_XLS_CDIAC105a, 2006.

Pytkowicz, R.: Calcium carbonate retention in supersaturated seawater, American Journal of Science, 273, 515-522, http://dx.doi.org/10.2475/ajs.273.6.515 1973.

Renforth, P. and Henderson, G.: Assessing ocean alkalinity for carbon sequestration, Reviews of Geophysics, 55, 636-674, https://doi.org/10.1002/2016rg000533, 2017.

Riebesell, U., Basso, D., Geilert, S., Dale, A. W., Kreuzburg, M., and Meysman, F.: Mesocosm experiments in ocean alkalinity enhancement research, State of the Planet Discussions, 2023, 1-21, https://doi.org/10.5194/sp-2-oae2023-6-2023, 2023.

Rogelj, J., Schaeffer, M., Friedlingstein, P., Gillett, N. P., van Vuuren, D. P., Riahi, K., Allen, M., and Knutti, R.: Differences between carbon budget estimates unravelled, Nature Climate Change, 6, 245-252, https://doi.org/10.1038/nclimate2868, 2016.

Sánchez, N., Goldenberg, S. U., Brüggemann, D., Weichler, M., Dorssers, S., and Riebesell, U.: Ecosystem impacts of Ocean Alkalization in an oligotrophic marine plankton community: A mesocosm study, Copernicus Meetings, https://doi.org/10.5194/egusphere-egu23-15436, 2023.

Schuiling, R. D. and Krijgsman, P.: Enhanced Weathering: An Effective and Cheap Tool to Sequester Co2, Climatic Change, 74, 349-354, https://doi.org/10.1007/s10584-005-3485-y, 2006.

Schulz, K. G., Bach, L. T., and Dickson, A. G.: Seawater carbonate system considerations for ocean alkalinity enhancement research, State of the Planet Discussions, 2023, 1-24, https://doi.org/10.5194/sp-2-oae2023-2-2023, 2023.

Sterling, S., Halfyard, E., Hart, K., Trueman, B., Grill, G., and Lehner, B.: Addition of Alkalinity to Rivers: a new CO2 Removal Strategy, ESS Open Archive, https://doi.org/10.22541/essoar.168380809.92137625/v1, 2023.

Turek, M. and Gnot, W.: Precipitation of magnesium hydroxide from brine, Industrial & engineering chemistry research, 34, 244-250, https://doi.org/10.1021/ie00040a025, 1995.

UNFCCC: Report of the Conference of the Parties to the United Nations Framework Convention on Climate Change (21st Session, 2015: Paris). Retrieved December. Vol. 4. 2015., 2015.

Vassallo, F., La Corte, D., Cancilla, N., Tamburini, A., Bevacqua, M., Cipollina, A., and Micale, G.: A pilot-plant for the selective recovery of magnesium and calcium from waste brines, Desalination, 517, https://doi.org/10.1016/j.desal.2021.115231, 2021.

Wurgaft, E., Steiner, Z., Luz, B., and Lazar, B.: Evidence for inorganic precipitation of CaCO3 on suspended solids in the open water of the Red Sea, Marine Chemistry, 186, 145-155, https://doi.org/10.1016/j.marchem.2016.09.006, 2016.

629 Wurgaft, E., Wang, Z. A., Churchill, J. H., Dellapenna, T., Song, S., Du, J., Ringham, M. C., Rivlin, T., and Lazar, B.: Particle
630   Triggered Reactions as an Important Mechanism of Alkalinity and Inorganic Carbon Removal in River Plumes,
631   Geophysical Research Letters, 48, 277, https://doi.org/10.1029/2021gl093178, 2021.

632 Yang, B., Leonard, J., and Langdon, C.: Seawater alkalinity enhancement with magnesium hydroxide and its implication for
633   carbon dioxide removal, Marine chemistry, https://doi.org/10.1016/j.marchem.2023.104251, 2023.

634 Zeebe, R. and Wolf-Gladrow, D.: CO2 in Seawater: Equilibrium, Kinetics, Isotopes, Elsevier Oceanography Book Series. 65,
635   Amsterdam, 361 pp.2001.

636 Zhu, T. and Dittrich, M.: Carbonate Precipitation through Microbial Activities in Natural Environment, and Their Potential in
637   Biotechnology: A Review, Front Bioeng Biotechnol, 4, 4, https://doi.org/10.3389/fbioe.2016.00004, 2016.

638